

## CORROSION BEHAVIOR OF COPPER–ALUMINA NANOCOMPOSITES IN DIFFERENT CORROSIVE MEDIA

D. SABER<sup>1</sup>, KH. ABD EL-AZIZ<sup>2</sup> & A. FATHY<sup>3</sup>

<sup>1</sup>Department of Materials Engineering, Faculty of Engineering, Zagazig University, Egypt

<sup>1,2</sup>Department of Mechanical Engineering, College of Engineering, Taif University, Saudi Arabia

<sup>3</sup>Department of Mechanical Design and Production Engineering, Faculty of Engineering, Zagazig University, Egypt

### ABSTRACT

The present study aims to investigate the corrosion behavior of the Cu–Al<sub>2</sub>O<sub>3</sub> nanocomposite, with various alumina contents, in both 3.5wt.% NaCl and 0.5 M H<sub>2</sub>SO<sub>4</sub> solutions using electrochemical technique. The Cu–Al<sub>2</sub>O<sub>3</sub> nanocomposites with different weight fractions of Al<sub>2</sub>O<sub>3</sub> were produced by powder metallurgy method. The Cu–Al<sub>2</sub>O<sub>3</sub> nanocomposite powders were prepared by mechanochemical technique. The structure and characteristics of the powders and composites produced from this route were examined by XRD, SEM, EDS and metallography. The results showed that, the alumina of nano-sized particles was formed and dispersed within the copper matrix. It was found that the Cu–15% Al<sub>2</sub>O<sub>3</sub> nanocomposite had the lowest corrosion resistance. All specimens exhibited lower corrosion current density in 3.5wt% NaCl solution than that in 0.5M H<sub>2</sub>SO<sub>4</sub> solution.

**KEYWORDS:** MMCs, Nanocomposites, Corrosion, Microstructural Analysis

### INTRODUCTION

Metal matrix nanocomposites are a new class of nanostructured materials which are consisting of nanoparticles used as reinforcements. Normally, micron-sized particles are used to improve the ultimate tensile and yield strength of metals. However, the ductility of MMCs significantly deteriorates by high ceramic particle concentration [1]. Aluminum oxide (Al<sub>2</sub>O<sub>3</sub>) which has been investigated for high temperature structural applications is a hard refractory ceramic because of its good strength and low coefficient of thermal expansion. In recent years, more attention has been focused on nano alumina powders for using in advanced engineering materials [2]. Studies on the synthesis and characterization of nano-scale alumina dispersed copper metal matrix composites have attracted the scientific interest in the recent years, because nanostructure-type materials are expected to have special physical and mechanical properties. In the copper–alumina system, the nano-scale Al<sub>2</sub>O<sub>3</sub> particulate dispersion can provide unique characteristics, such as high thermal and electrical conductivities, as well as high strength and excellent resistance to high temperature annealing. Therefore, Cu-based metal matrix composites are being used in many industrial applications such as; contact supports, frictional break parts, electrode materials for lead wires and spot welding [3, 4]. The main requirements for structure of these materials are a homogenous distribution and small size of oxide particles on copper matrix [5, 6]. Many manufacturing processes have been used for producing such composites. In general, most metal matrix composites are produced by squeeze or stir casting or by spray forming or by powder metallurgy techniques. In these methods the reinforcements are incorporated or added into the matrix by ex-situ methods. Recently, in-situ chemical process is adopted to produce the Cu–Al<sub>2</sub>O<sub>3</sub> nanocomposite powder with a homogenous distribution of oxide particles in the copper matrix.

The in-situ method in which the reinforcements are created by chemical reactions during composite fabrication has been employed in this study. Mechanochemical milling has been used to eliminate agglomeration of reinforcements and to obtain dispersed nanoparticles [7, 8]. However, the mechanisms responsible for the in-situ formation of reinforcement phases in some reaction systems are not well understood [9–11]. The in-situ chemical process has several advantages over the other methods such as; more homogenous reinforcement, excellent surface bonding and pure inter-phase. Therefore, it appears to be a suitable method for preparing Cu–Al<sub>2</sub>O<sub>3</sub> nanocomposite [12–16].

In spite of the extensive research for development of the physical and mechanical properties of MMCs, few studies have been devoted to their corrosion behavior [17]. The effect of reinforcements on corrosion behavior of composites is still unclear. Corrosion current density has been shown to increase, decrease or remaining unaffected in the presence of reinforcements. In addition, reinforcements have been shown to increase or decrease or not to affect the open circuit potential (OCP) [18]. The main causes of the corrosion in MMCs are reported as; (1) galvanic coupling between the matrix and the reinforcement materials, (2) formation of an interfacial phase between the reinforcement and matrix and (3) microstructural changes resulted from manufacture of the MMCs [19–21]. The objective of the present work is to study the effect of Al<sub>2</sub>O<sub>3</sub> nanoparticles contents on the corrosion behavior of the produced nanocomposites.

## EXPERIMENTAL WORK

The Cu–Al<sub>2</sub>O<sub>3</sub> nanocomposite powders containing different alumina contents were prepared by mechanochemical technique, in which copper powder and aluminum nitrate Al(NO<sub>3</sub>)<sub>3</sub> were used as transient components. Cu–Al<sub>2</sub>O<sub>3</sub> nanocomposite briquettes were fabricated by cold pressing at 600 MPa then sintering at 950°C in a hydrogen atmosphere for 2 hours as reported in details elsewhere [22]. X-ray diffractometer with Cu K $\alpha$  radiation was used to assess the transformation of the phases and to measure the crystallite size of nanocomposite powders [23]. Nanocomposite powders were examined using scanning electron microscopy (SEM) with energy dispersive spectrometer (EDS). Microstructural examination was conducted on metallographically polished samples to investigate the morphological characteristics of the grains and present phases.

The corrosion behavior of Cu–Al<sub>2</sub>O<sub>3</sub> nanocomposites was studied in 3.5 wt.% NaCl and 0.5 M H<sub>2</sub>SO<sub>4</sub> solutions using electrochemical techniques. Both 3.5 wt.% NaCl and 0.5 M H<sub>2</sub>SO<sub>4</sub> solutions were prepared prior to each test using distilled water. All electrochemical experiments were conducted using a Gamry PCI300/4 Potentiostat/Galvanostat/ZRA analyzer connected to a PC. The Echem Analyst software (version 5.21) was used for all electrochemical data analysis. A three-electrode cell composed of a specimen as a working electrode, platinum counter electrode and saturated calomel electrode (SCE) as a reference electrode was used for the tests. Tafel polarization tests were carried out using a scan rate of 0.5 mV/min at 25°C. The specimens with exposed surface area of 1.0 cm<sup>2</sup> were used as a working electrode. Prior to electrochemical tests, the specimens were cathodically cleaned for 15 min at -1500 mV (SCE) to remove the air-formed oxide film. The applied routine automatically selects the data that lies within the Tafel region ( $\pm 250$  mV with respect to the corrosion potential).

## RESULTS AND DISCUSSIONS

### Microstructure and Phase Analysis

Figure 1 shows X-ray diffraction (XRD) pattern of the produced nanocomposite (Cu–15% Al<sub>2</sub>O<sub>3</sub>) powder (after reduction by hydrogen). Peaks of elementary Cu and Al<sub>2</sub>O<sub>3</sub> are quite pronounced in the pattern, confirming the

formation of  $\text{Al}_2\text{O}_3$ . However the intensity of the  $\text{Al}_2\text{O}_3$  peaks is very low and not up to the proportion of the 15 wt. %  $\text{Al}_2\text{O}_3$ . The reason for this may be attributed to the facts that the  $\text{Al}_2\text{O}_3$  nanoparticles are extremely small and that they are embedded in a Cu matrix which has high density [22]. The particle size of alumina, ( $\text{Al}_2\text{O}_3$ ) was calculated from X-ray line broadening using Scherer's formula ( $D = 0.9\lambda / B \cos \theta$ ), where, D is the crystallite size,  $\lambda$  is the wavelength of the radiation,  $\theta$  is the Bragg's angle and B is the full width at half maximum [23]. The size of alumina nanoparticles showed a value of 50 nm whilst size of copper crystallites were 200 nm.

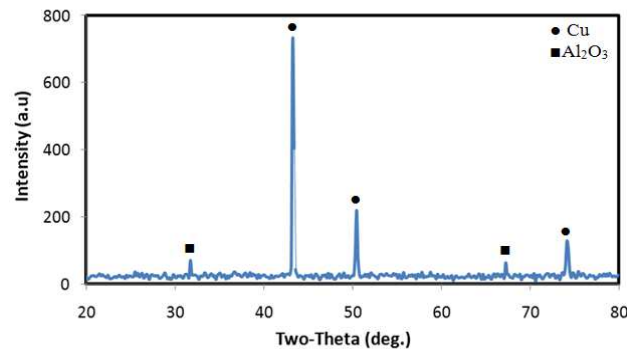


**Figure 1: X-Ray Diffraction Patterns of (Cu–15%Al<sub>2</sub>O<sub>3</sub>) Composite Powder**

The obtained Cu- $\text{Al}_2\text{O}_3$  powders were characterized by scanning electron microscopy (SEM) with an energy spectrum analyzer (EDS) as presented in Figure 2. Microstructural analysis of the powders confirmed the possibility of Cu- $\text{Al}_2\text{O}_3$  nanocomposite synthesis by the mechanochemical technique, starting from copper powder and aqueous solution of  $\text{Al}(\text{NO}_3)_3$ . The surface morphology is rough. EDS image scan indicates that uniform distribution of Cu, Al and O elements all over surface. The level of copper is much higher than that of aluminum and oxygen.

For the composite materials, it is very important to obtain homogeneous reinforcement in the matrix in order to enhance mechanical, electrical and thermal properties. Figure 3 shows optical microstructure of polished Cu- $\text{Al}_2\text{O}_3$  nanocomposite with 10%  $\text{Al}_2\text{O}_3$  fabricated by mechanochemical technique after sintering at 950 °C for 2 h in hydrogen. The microstructure is composed of fine Cu and  $\text{Al}_2\text{O}_3$ . There are two distinct regions; one region is a black area representing alumina, the other one is a white area mostly occupied by copper. It can be noted that the alumina phase (dark regions) is relatively good distributed in copper matrix. In order to indicate the distribution of elements in the structure, surface analysis of a polished sintered sample containing 10%  $\text{Al}_2\text{O}_3$  was performed by both SEM and EDS. The composition scanning (EDS) images shown in Figure 4 shows a homogeneous distribution of elements in the structure. It can be seen that copper covers almost the entire surface of the sample. The results of surface scanning for aluminum and oxygen show that these two elements are present less in the structure of the sintered sample and the surfaces they occupy are inter-lapping, which corresponds to the existence of an  $\text{Al}_2\text{O}_3$  dispersed in the structure.

## CORROSION BEHAVIOR OF CU– $\text{Al}_2\text{O}_3$ NANOCOMPOSITES

### Corrosion behavior in 3.5wt% NaCl Solution

Polarization curves of the pure copper specimens and the composite samples in 3.5% NaCl solution are given in Figure 5. Corrosion potential and current density values were also calculated by Tafel extrapolation method and listed in Table 1. Figure 5 shows the striking similarity between typical polarization curves for the composite specimens and the pure copper specimen. The behavior exhibited by the composites is therefore consistent with that of pure copper in chloride media as detailed by Lee et al [25] and Milsevet al [26]. The anodic polarization

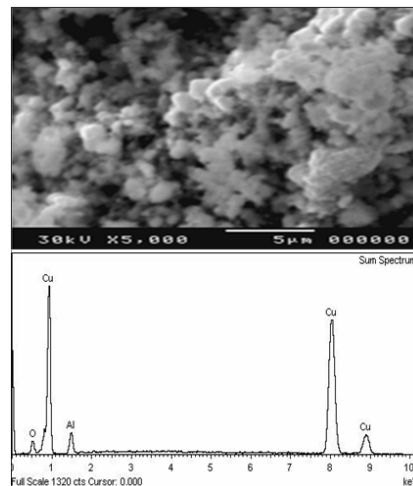


**Figure 2: SEM and EDS Analysis Micrograph of the (Cu–15%Al<sub>2</sub>O<sub>3</sub>) Nanocomposite Nanocomposite Powders**

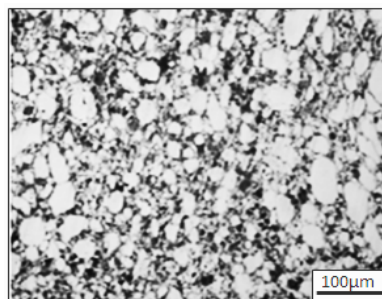


**Figure 3: Microstructure of Nanocomposite Containing 10% Al<sub>2</sub>O<sub>3</sub>**

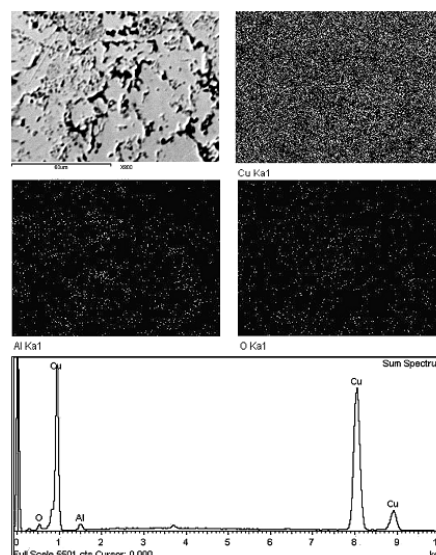


**Figure 4: Sem Image and Eds Composition Scanning of Cu, Al and O for (Cu–10%Al<sub>2</sub>O<sub>3</sub>) Nanocomposite, Showing the Very Uniform Distribution of the Elements**

behavior of the copper composites is dependent on the mass transport-reaction mechanisms of the chloride ions. A model to explain the anodic polarization characteristics of Cu has been proposed [27] and is described below. Considering the anodic reaction in chloride media, the corrosion process involves at least three steps: (a) transport of chloride ions to the Cu/NaCl solution interface, (b) reactions at the interface as shown in equations (2) and (3), and (c) transport of the

corrosion products away from the interface or deposition of the products on the Cu surface. Each of these reactions has its own rate-limiting step.

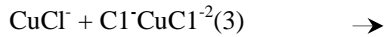
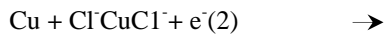


**Table 1: Corrosion Properties of (Cu–Al<sub>2</sub>O<sub>3</sub>) Nanocomposite with Different Al<sub>2</sub>O<sub>3</sub> Content in 3.5%NaCl Solution**

Composites	Corrosion Current Density $I_{\text{corr}}$ (Ma/Cm <sup>2</sup> )	Corrosion Potential $E_{\text{corr}}$ (- Mv)
Cu	0.012	213
(Cu–10%Al <sub>2</sub> O <sub>3</sub> )	0.039	223
(Cu–15%Al <sub>2</sub> O <sub>3</sub> )	0.063	163

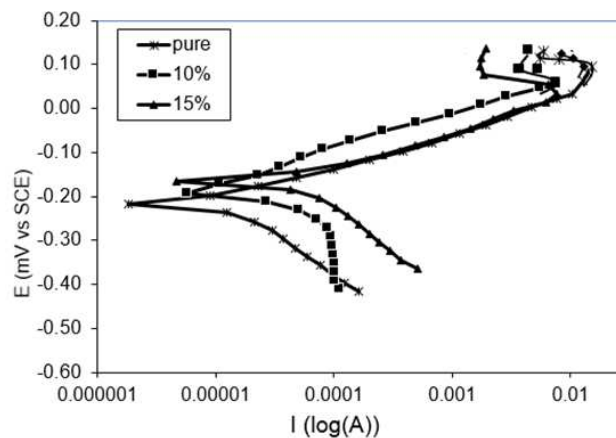


**Figure 5: Potentiodynamic Polarization Curves for (Cu–Al<sub>2</sub>O<sub>3</sub>) Nanocomposite in 3.5wt.% NaCl Solution**

It can be seen from Table 1 that the corrosion current density ( $i_{\text{corr}}$ ) value of the pure copper specimen increased by Al<sub>2</sub>O<sub>3</sub> nano particle addition. It was found that the  $i_{\text{corr}}$  of pure copper was 0.012 mA/cm<sup>2</sup> and the addition of 10% Al<sub>2</sub>O<sub>3</sub> led to increase in current density registered 0.039 mA/cm<sup>2</sup>. On the other hand, the severity of corrosive attack increased with 15 wt.% Al<sub>2</sub>O<sub>3</sub> (0.063 mA/cm<sup>2</sup>). As shown in Table (1) the corrosion potential ( $E_{\text{corr}}$ ) of pure copper was -213 mV. While  $E_{\text{corr}}$  of the (Cu–Al<sub>2</sub>O<sub>3</sub>) nanocomposite was -223 mV for the specimen with 10% Al<sub>2</sub>O<sub>3</sub> and -163 mV for the specimen with 15% Al<sub>2</sub>O<sub>3</sub>. From these observations, it seems that the (Cu–Al<sub>2</sub>O<sub>3</sub>) nanocomposite have less corrosion resistance as compared to the pure copper. One possible reason for this is that the (Cu–Al<sub>2</sub>O<sub>3</sub>) nanocomposite may have a higher initial susceptibility to corrode compared to pure copper because of the presence of Al<sub>2</sub>O<sub>3</sub> particles. The (Cu–Al<sub>2</sub>O<sub>3</sub>) nanocomposite may corrode in the interfacial area due to the residual stresses between the alumina particles and the copper matrix. In other words, it may be easy to initiate corrosion in the (Cu–Al<sub>2</sub>O<sub>3</sub>) nanocomposite [28].

#### Corrosion behavior in 0.5M H<sub>2</sub>SO<sub>4</sub> Solution

Polarization curves of the base Cu and the composite samples in 0.5M H<sub>2</sub>SO<sub>4</sub> solution are given in Figure 6. Corrosion potential and current density values were given in Table (2). As shown in Figure 6, (Cu–Al<sub>2</sub>O<sub>3</sub>) nanocomposite with different weight percentage of Al<sub>2</sub>O<sub>3</sub> showed nearly the same behavior in both anodic and cathodic regions. It can be seen from Table (2) that the corrosion current density ( $i_{\text{corr}}$ ) value of the pure copper specimen was increased by Al<sub>2</sub>O<sub>3</sub> nano particles addition. The  $i_{\text{corr}}$  of (Cu–10 % Al<sub>2</sub>O<sub>3</sub>) nanocomposite and pure copper was (0.354 and

0.246 mA/cm<sup>2</sup>) respectively. The highest attack of tested specimens had taken place in case of (Cu– 15% Al<sub>2</sub>O<sub>3</sub>) nanocomposite (5.3 mA/cm<sup>2</sup>). As shown in Table 2, there is a difference in the corrosion potential ( $E_{corr}$ ) between the (Cu–Al<sub>2</sub>O<sub>3</sub>) nanocomposite and the pure copper. The corrosion potential was 63.6 mV in case of (Cu– 15%Al<sub>2</sub>O<sub>3</sub>) nanocomposite, while it was 29.5 mV in case of pure copper.

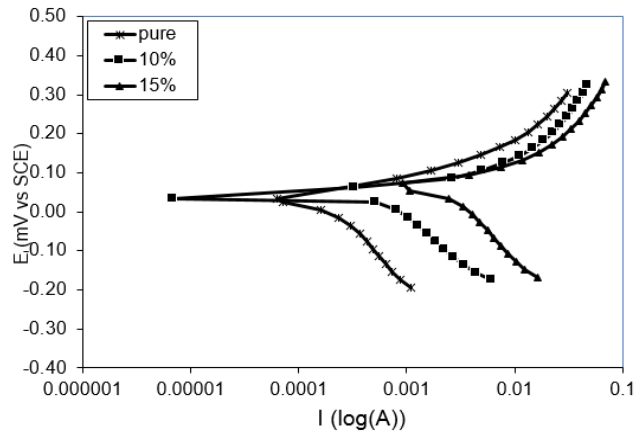


**Figure 6: Potentiodynamic Polarization Curves for (Cu–Al<sub>2</sub>O<sub>3</sub>) Nanocomposite in 0.5m H<sub>2</sub>so<sub>4</sub> Solution**

**Table 2: Corrosion Properties of (Cu–Al<sub>2</sub>O<sub>3</sub>) Nanocomposite with Different Al<sub>2</sub>O<sub>3</sub> Content in 0.5M H<sub>2</sub>SO<sub>4</sub> Solution**

Composites	Corrosion Current Density $I_{corr}$ (Ma/Cm <sup>2</sup> )	Corrosion Potential $E_{corr}$ (Mv)
Cu	0.246	29.5
(Cu–10% Al <sub>2</sub> O <sub>3</sub> )	0.354	32.9
(Cu–15% Al <sub>2</sub> O <sub>3</sub> )	5.3	63.6

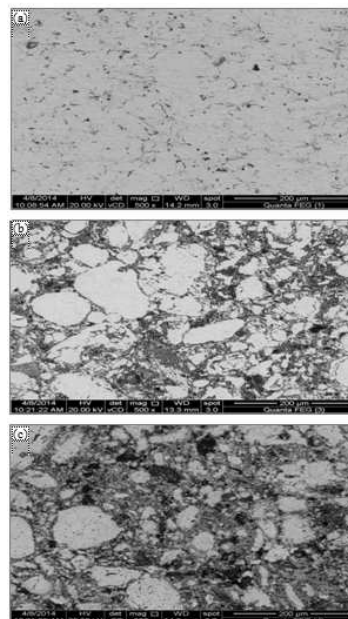


**Figure 7: SEM Micrographs of Corroded Surfaces after potentiodynamic polarization measurement in 3.5% NaCl solution (a) Pure Cu, (b) Cu–10%Al<sub>2</sub>O<sub>3</sub>, and (c) Cu–15%Al<sub>2</sub>O<sub>3</sub>**



By comparing the results of corrosion behavior in 3.5wt.% NaCl solution and that in 0.5M H<sub>2</sub>SO<sub>4</sub> solution, it can be seen that the corrosion current density  $i_{\text{corr}}$  of all specimens is increased in 0.5M H<sub>2</sub>SO<sub>4</sub> solution in comparison with 3.5wt.% NaCl. This result may be due to a high rate of dissolution of the specimens in 0.5M H<sub>2</sub>SO<sub>4</sub> solution in comparison with 3.5wt.% NaCl [29]. It can be also noted that there was a gradual increase in  $i_{\text{corr}}$  values of (Cu–10% Al<sub>2</sub>O<sub>3</sub>) nanocomposite compared to the pure copper specimens in 3.5wt.% NaCl solution as well as in 0.5M H<sub>2</sub>SO<sub>4</sub> solution. While there was a severely increase in  $i_{\text{corr}}$  values of (Cu–15% Al<sub>2</sub>O<sub>3</sub>) nanocomposite compared to the pure copper specimens in 0.5M H<sub>2</sub>SO<sub>4</sub> solution. This behavior is associated with the very uniform distribution of Al<sub>2</sub>O<sub>3</sub> in (Cu–10%Al<sub>2</sub>O<sub>3</sub>) nanocomposite and good connection of the matrix with the reinforcement particles [30,31].

Corrosion of (Cu–Al<sub>2</sub>O<sub>3</sub>) nanocomposite may be influenced by microstructural features due to the presence of the reinforcements, and intermetallic phases that may be formed around reinforcements [24]. Differences in the coefficient of thermal expansion between reinforcements and matrices can lead to the generation of dislocations [32] during heating and cooling of (Cu–Al<sub>2</sub>O<sub>3</sub>) nanocomposite. High dislocation density may possibly lead to higher corrosion in some metals [33]. The reinforcement particles left in relief resulting from matrix corrosion may form fissures, leading to crevice-type corrosion [34, 35]. Intermetallic phases may have potentials and corrosion resistances different from the matrix [36]. Active intermetallics and those with high corrosion rates may corrode and leave fissures or crevices on dissolution.

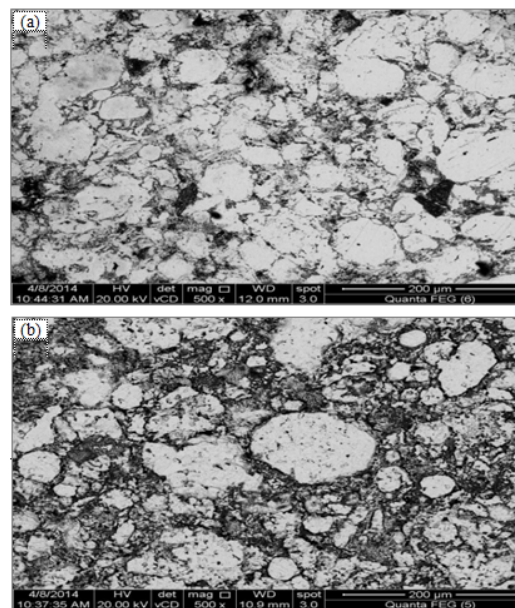


**Figure 8: SEM Micrographs of Corroded Surfaces after Potentiodynamic Polarization Measurement in 0.5M H<sub>2</sub>SO<sub>4</sub> Solution (A) Cu–10%Al<sub>2</sub>O<sub>3</sub>; (B) Cu–15%Al<sub>2</sub>O<sub>3</sub>**

#### **Microstructure Characteristics of the Corroded Surfaces after Corrosion**

The corroded surfaces of the base Cu and the composite samples after polarization test in 3.5% NaCl solution were exhibited in Figure 7(a-c). Pure copper has the best corrosion resistance and its corroded surface is shown in Figure 7-a. It can be observed that the corrosion of pure copper is a uniform corrosive damage. Comparing Figure 7-b and Figure 7-c, it is clear that the corroded surfaces of (Cu–15%Al<sub>2</sub>O<sub>3</sub>) nanocomposite is more rough than that of specimen (Cu–10%Al<sub>2</sub>O<sub>3</sub>) nanocomposite. As the Al<sub>2</sub>O<sub>3</sub> increased in copper matrix, imperfections were introduced due to different coefficient of thermal expansion between Al<sub>2</sub>O<sub>3</sub> and Cu. The interface becomes weak and it will be a preferred site for corrosion attacking, therefore, crevice corrosion happens easily. Corroded surfaces of (Cu–10%Al<sub>2</sub>O<sub>3</sub>) nanocomposite and

(Cu–15% Al<sub>2</sub>O<sub>3</sub>) nanocomposite after polarization test in 0.5M H<sub>2</sub>SO<sub>4</sub> solution were shown in Figure 8(a,b). As shown in Figure 8-a, the corroded surface seems plainer than that of (Cu–15% Al<sub>2</sub>O<sub>3</sub>) nanocomposite Figure 8-b. There are many depressions on the corroded surface of (Cu–15% Al<sub>2</sub>O<sub>3</sub>) nanocomposite where Al<sub>2</sub>O<sub>3</sub> particles were pulled out from the copper matrix. The corroded surface proves that there is some serious corrosion which results in debonding of Al<sub>2</sub>O<sub>3</sub> on the interfaces between copper and Al<sub>2</sub>O<sub>3</sub>. The ability of the matrix to tightly bond with the reinforcement is poor, and inevitably, Al<sub>2</sub>O<sub>3</sub> particles are more easily pulled out from the matrix.

## CONCLUSIONS

In the present study, the corrosion behavior of copper–alumina nanocomposites in NaCl, and H<sub>2</sub>SO<sub>4</sub> was investigated. The main conclusions drawn from the current study were:

- The potentiodynamic polarization curves generated for pure copper and (Cu–Al<sub>2</sub>O<sub>3</sub>) nanocomposite were similar. The four regions of polarization behavior, typical of pure copper, were observed in 3.5wt.% NaCl solution.
- In both 3.5wt.% NaCl and 0.5M H<sub>2</sub>SO<sub>4</sub> solutions, the severity of the corrosion of the (Cu–Al<sub>2</sub>O<sub>3</sub>) nanocomposite increased with increasing Al<sub>2</sub>O<sub>3</sub> content.
- Addition of 10 wt.% Al<sub>2</sub>O<sub>3</sub> showed small rise in  $i_{\text{corr}}$  of pure copper as compared with addition of 15 wt.% Al<sub>2</sub>O<sub>3</sub> in both 3.5wt.% NaCl and 0.5M H<sub>2</sub>SO<sub>4</sub> solutions.
- All specimens exhibited corrosion current density in 3.5wt% NaCl solution lower than that in 0.5M H<sub>2</sub>SO<sub>4</sub> solution.

## ACKNOWLEDGEMENTS

The authors would like to thank Prof. Adel A. Omar, Professor of material science, Benha University and Taif University for his valuable discussion and comments.

## REFERENCES

1. A. Mazahery, H. Abdizadeh, H. R. Baharvandi, "Development of high performance A356/nano-Al<sub>2</sub>O<sub>3</sub> composites", Mater. Sci. Eng. A, Vol. 61, pp.518, (2009).
2. I. Zamblau, C. Varvara, L. M. Muresana, "Corrosion behavior of composite coatings obtained by electrolytic codeposition of copper with Al<sub>2</sub>O<sub>3</sub> nanoparticles", Chem. Biochem. Eng. Q., Vol. 23, pp.43, (2009).
3. A. Fathy and Omya El-Kady, "Thermal expansion and thermal conductivity characteristics of Cu–Al<sub>2</sub>O<sub>3</sub> nanocomposites", Materials and Design, Vol.46, pp.355, (2013).
4. A. Krüger and A. Mortensen, "In situ copper–alumina composites", Materials Science & Engineering A, Vol. 585, pp.396, (2013).
5. P. K. Jena, E. A. Brocchi, I. G. Solórzano, M. S. Motta, "Identification of a third phase in Cu–Al<sub>2</sub>O<sub>3</sub> nanocomposites prepared by chemical routes", Mater. Sci. Eng. A, Vol. 72, pp.371, (2004).
6. S. H. Kim, D. N. Lee, "Technical note fabrication of alumina dispersion strengthened copper strips by internal oxidation and hot roll bonding", Mater. Sci. Technol., Vol. 15, pp.352, (1999).



7. M. Karbalaee Akbari, O. Mirzaee, H.R. Baharvandi, "Fabrication and study on mechanical properties and fracture behavior of nanometric  $\text{Al}_2\text{O}_3$  particle-reinforced A356 composites focusing on the parameters of vortex method", *Materials and Design*, Vol.46, pp.199, (2013).
8. D.Y. Ying and D.L. Zhang, "Processing of Cu– $\text{Al}_2\text{O}_3$  metal matrix nanocomposite materials by using high-energy ball milling", *Mater. Sci. Eng. A*, Vol.152, pp.226, (2000).
9. P. Yu, Ch. J. Deng, N. G. Ma, M. Y. Yau, "Formation of nanostructured eutectic network in  $\text{Al}_2\text{O}_3$  reinforced Al–Cu alloy matrix composite", *Acta Mater*, Vol. 51, pp.3445, (2003).
10. J. P. Tu, N. Y. Wang, Y. Z. Yang, F. Liu, X. B. Zhang, "Preparation and properties of  $\text{TiB}_2$  nanoparticle reinforced copper matrix composites by in situ processing", *Mater. Lett.*, Vol. 52, pp.448, (2002).
11. H. X. Lu, J. Hu, Ch. P. Chen, H. Wei, "Characterization of  $\text{Al}_2\text{O}_3$ –Al nano-composite powder prepared by a wet chemical method", *Ceram. Int.*, Vol. 31, pp.481, (2005).
12. Ding Jian, Zhao Naiqin, Shi Chunsheng, and Li Jiajun, "In situ formation of Cu– $\text{ZrO}_2$  composites by chemical routes", *J Alloy Compd.*, Vol. 425, pp.390, (2006).
13. D. W. Lee, G. H. Ha, B. K. Kim, "Synthesis of Cu– $\text{Al}_2\text{O}_3$  nano-composite powder", *Scripta Mater.*, Vol. 44, pp.2137, (2001).
14. M. S. Motta, P. K. Jena, E. A. Brocchi, "Characterization of Cu– $\text{Al}_2\text{O}_3$  nano-scale composites synthesized by in situ reduction", *Mater. Sci. Eng. C*, Vol. 15, pp.175, (2001).
15. P. K. Jena, E. A. Brocchi, M. S. Motta, "In situ formation of Cu– $\text{Al}_2\text{O}_3$  nano-scale composites by chemical routes and studies on their microstructures" *Mater. Sci. Eng. A*, 313:180, (2001).
16. M. Entezarian, R. A. Drew, "Direct bonding of copper to aluminum nitride", *Mater. Sci. Eng. A*, Vol. 212, pp.206, (1996).
17. Sennur Candan, "An investigation on corrosion behaviour of pressure infiltrated Al–Mg Alloy/ $\text{SiC}_p$  composites", *Corrosion Science*, Vol. 51, pp.1392, (2009).
18. D. G. Kolman, D. P. Butt, "Corrosion behavior of a novel  $\text{SiC}/\text{Al}_2\text{O}_3/\text{Al}$  composite exposed to chloride environments", *Journal of the Electrochemical Society*, Vol. 144, pp.3785, (1997).
19. S. Winkler, H. Flower, "Stress corrosion cracking of cast 7XXX aluminium fibre reinforced composites", *Corrosion Science*, Vol.46, pp.903, (2004).
20. B. Bobic, S. Mitrovic, M. Babic, I. Bobic, "Corrosion of aluminium and zinc–aluminium alloys based metal–matrix composites", *Tribology in Industry*, Vol. 31, pp.44, (2009).
21. F. Toptan, A. C. Alves, I. Kerti, E. Ariza, L. A. Rocha, "Corrosion and tribo corrosion behavior of Al–Si–Cu–Mg alloy and its composites reinforced with  $\text{B}_4\text{C}$  particles in 0.05 M NaCl solution", *Wear*, Vol. 306, pp.27, (2013).
22. F. Shehata, A. Fathy, M. Abdelhameed and S. Moustafa, "Preparation and properties of  $\text{Al}_2\text{O}_3$  nanoparticle reinforced copper matrix composites by in situ processing", *Materials & Design*, Vol. 30(7), pp.2756, (2009).
23. B. D. Cullity, "Elements of X-ray diffraction", 2<sup>nd</sup> ed. California, USA: Addison- Wesley; p. 102, (1978).

24. L. H. Hihara, "Corrosion of Metal-Matrix Composites", Handbook, Vol. 13B:Corrosion: Materials S.D. Cramer, B. S. Covino, Jr., editors, p526-542.
25. H. P. Lee, K. Nobe, "Kinetics and mechanisms of Cu electrodisolution in Chloride Media", J. Electrochemical Soc., Vol.133, pp.2035, (1986).
26. I. Milosev, M. Metikos-Hukovic, "Passive films on 90Cu–10Ni Alloy: The mechanism of breakdown in chloride containing solutions", J. Electrochem. Soc., Vol. 138, pp.61, (1991).
27. W.D. Bjorndahl, K. Nobe, "Copper corrosion in chloride media effect of oxygen", Corrosion, Vol. 40, pp.82, (1984).
28. Harovel G. Wheat, "Corrosion behavior of metal matrix composites" Final Report For The Period July 1, 1989 Through September (1992).
29. K. K. Alaneme, M. O. Bodunrin, "Corrosion behavior of alumina reinforced aluminum (6063) metal matrix composites" Journal of Minerals & Materials Characterization & Engineering, Vol.10, pp.1153, (2011).
30. Khalid Abd El-Aziz, Dalia Saber, Hossam El-Din M. Sallam, "Wear and corrosion behavior of Al–Si matrix composite reinforced with alumina", Journal of Bio- and Tribo-Corrosion, Vol. 1(5), (2015).
31. L. A. Dobrzanski, A. Włodarczyk, M. Adamiak, "Structure, properties and corrosion resistance of PM composite materials based on EN AW-2124 aluminum alloy reinforced with the Al<sub>2</sub>O<sub>3</sub> ceramic particles", Journal of Materials Processing Technology, Vol. 27, pp.162, (2005).
32. R. J. Arsenault, "In metal matrix composites: mechanisms and properties", R.K. Everett and R.J. Arsenault, Ed., Academic Press, pp.79, (1991).
33. H. H. Uhlig, R.W. Revie, "Corrosion and corrosion control", 3<sup>rd</sup> ed., John Wiley and Sons, Inc., Vol. 354, pp.123, (1985).
34. L. H. Hihara, Z.J. Lin, "Corrosion of Silicon/Aluminum metal-matrix composites", Sixth Japan International SAMPE Symposium and Exhibition, pp.26–29 (Tokyo, Japan), Society for the Advancement of Material and Process Engineering, (1999).
35. L. H. Hihara, H. Ding, T. Devarajan, "Corrosion-initiation sites on aluminum metal-matrix composites," U.S. Army Corrosion Summit, (Cocoa Beach, FL), U.S. Army, 2004.
36. E. H. Hollingsworth and H.Y. Hunsicker, in Corrosion, Vol 13, ASM Handbook, ASM International, pp.583, (1987).